Supporting Information for

New Soft-matter Material with Old Chemistry: Passerini Multicomponent Polymerization-induced Assembly of An AIE-active Double-helical Polymer with Rapid Visible-light Degradability

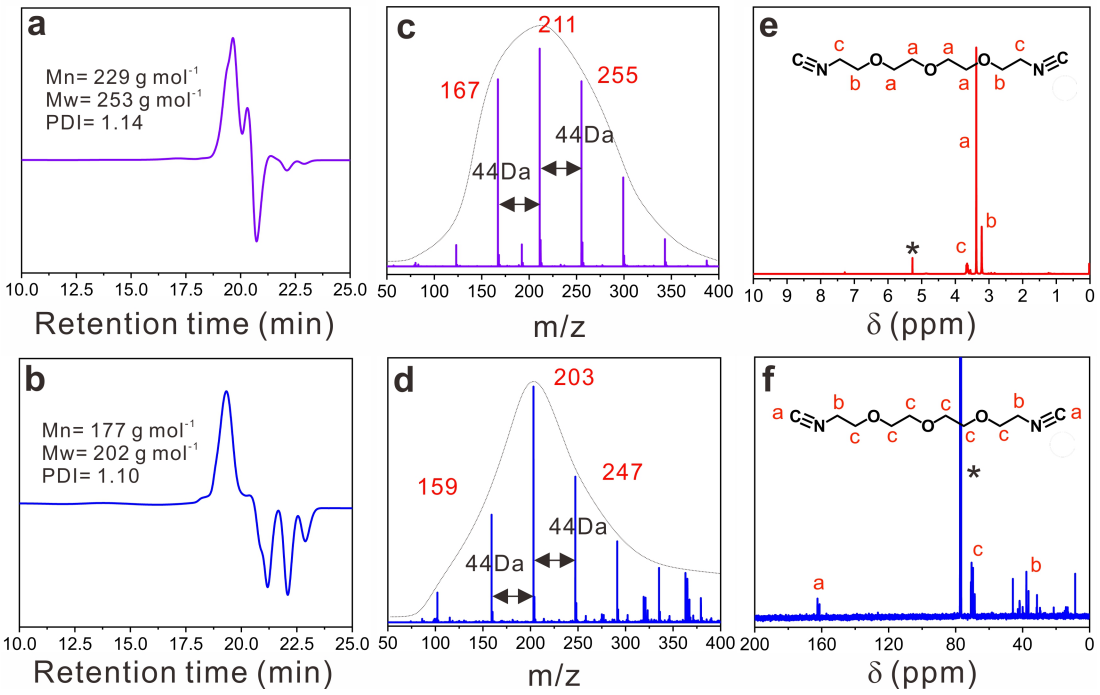

Figure S1. GPC curves and mass spectra of (a, c) commercialized HOOC-PEG-COOH and (b, d) as-synthesized NC-PEG-CN. (e) ^{1}H-NMR and (f) ^{13}C-NMR spectra of as-synthesized NC-PEG-CN.

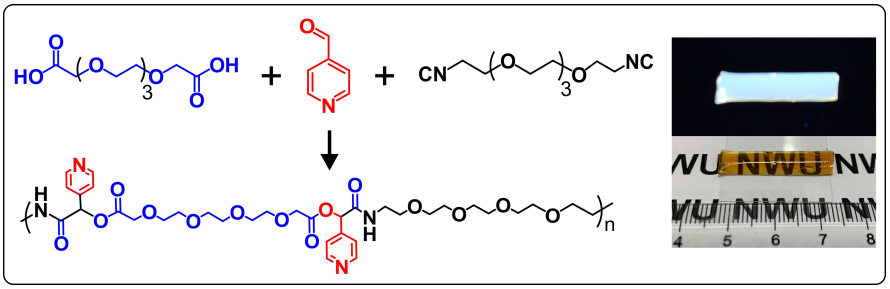

Figure S2. Synthesis of WADP via the PMPIA strategy in DMF or THF, and the dried sample under white and UV light irradiation.

Table 1 Synthesis conditions listed of WADP

polymer	solvent	molar ratio	conc. (M)	time (d)	Mn (x10^4)	PDI
P1	THF	1:2:1	1.6	2.5	1.5	2.3
P2	THF	1:2:1	0.8	4	1.3	2.5
P3	THF	1:2:1	0.8	2.5	1.7	2.0
P4	DMF	1:2:1	0.8	4	1.2	2.1
P5	THF	1:3:1	0.8	2.5	0.9	1.7
P6	**THF**	**1:2:1**	**1.6**	**3**	**1.8**	**2.0**

Note: The molar concentration listed in each case is the total concentration of HOOC-PEG-COOH, PyCHO and CN-PEG-NC. The molar ratio is $n_{HOOC\text{-}PEG\text{-}COOH}$: n_{PyCHO} : $n_{CN\text{-}PEG\text{-}NC}$.

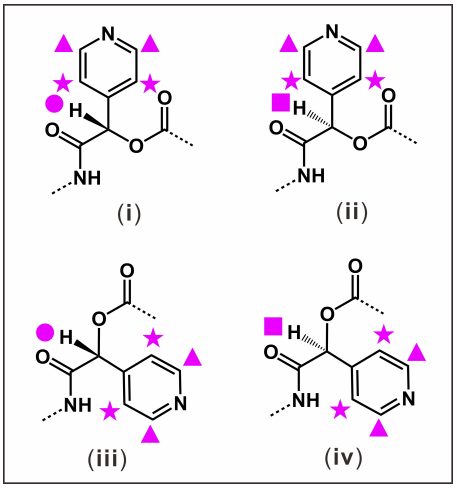

Figure S3. The chiral structures of pyridine units in the as-prepared WADP polymers.

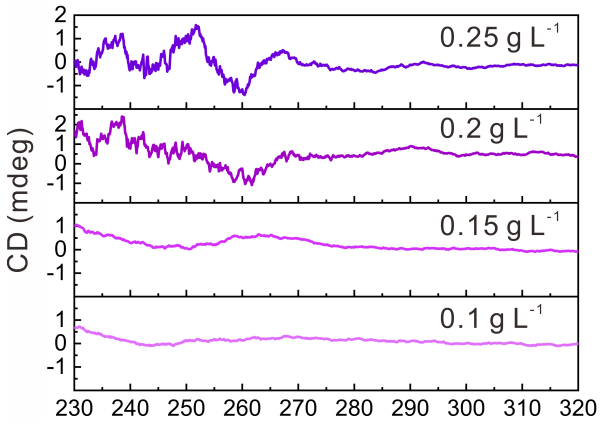

Figure S4. Circular dichroism characterization of WADP with different concentrations in DMSO.

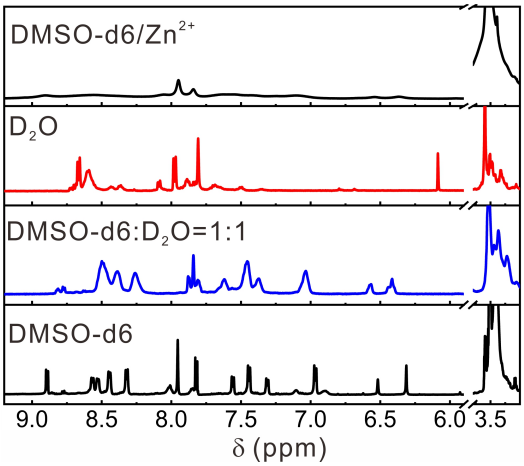

Figure S5. ^{1}H-NMR spectra of WADP in DMSO-d6, DMSO-d6/D_2O, D_2O, and DMSO-d6/Zn^{2+}.

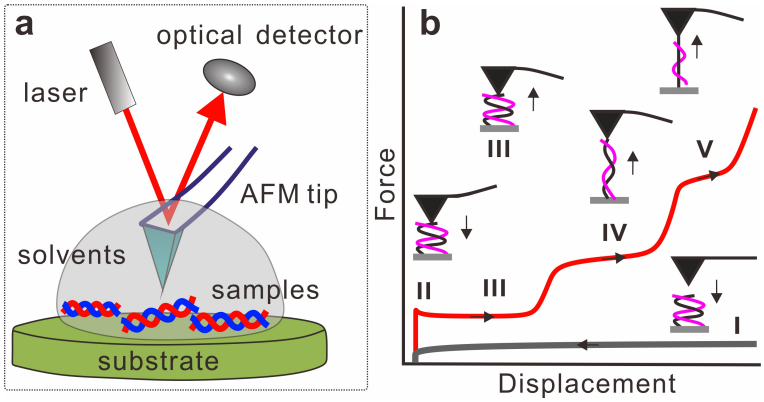

Figure S6. (a) The schematic illustration of single-molecule force spectroscopy for in situ studying the conformational transitions in helical polymers. (b) The corresponding conformations of polymers during the characterization process.

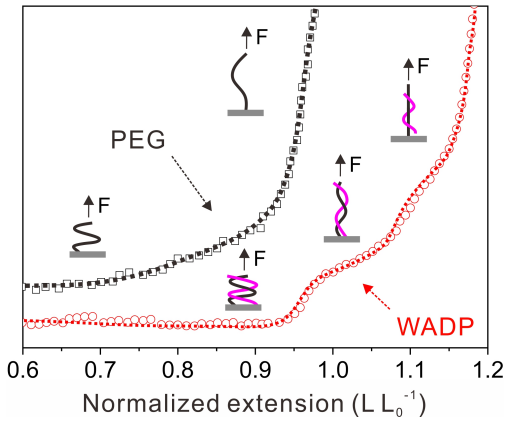

Figure S7. Single-molecule force spectroscopy characterization of PEG and WADP in water.

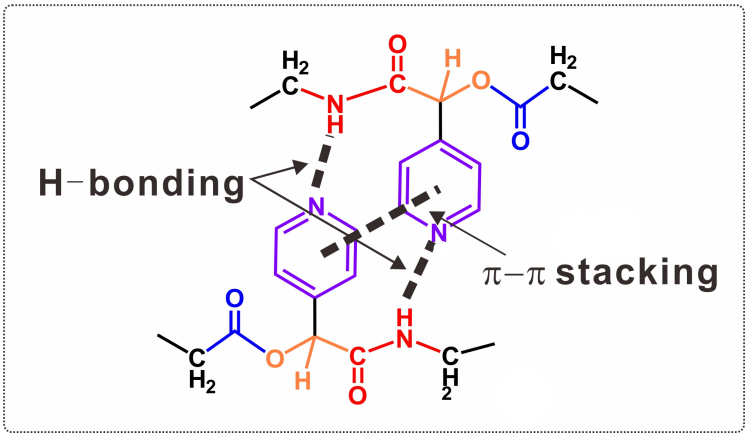

Figure S8. Schematic illustration of supramolecular interactions in the helical WADP.

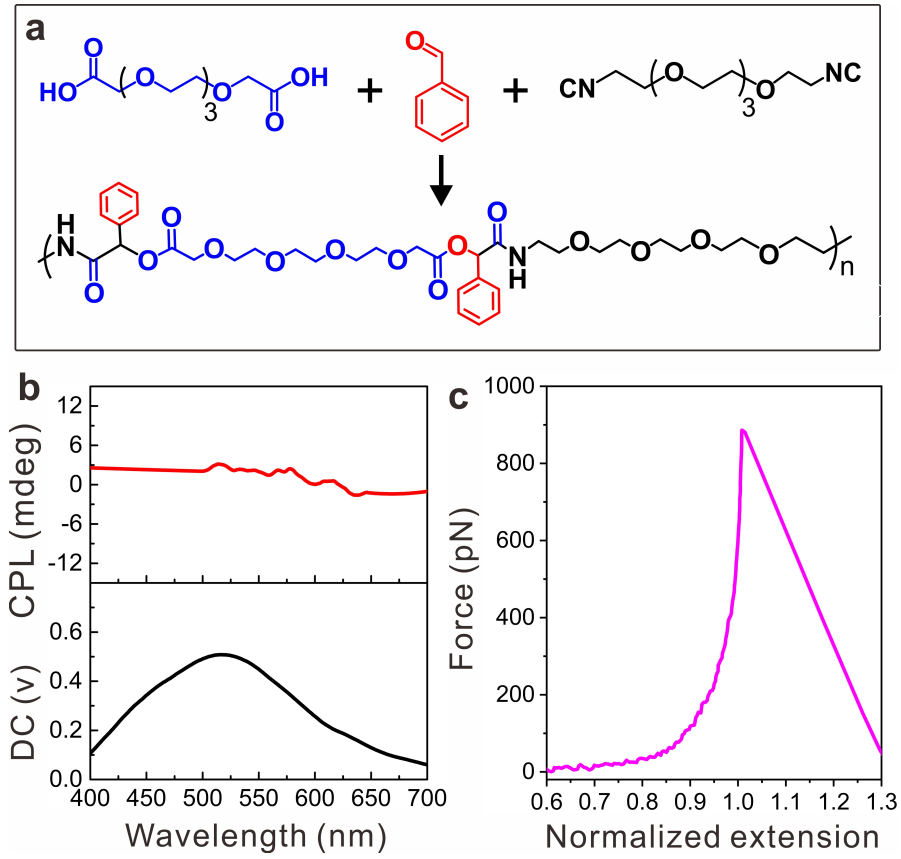

Figure S9. (a) Synthesis of control polymer by using benzaldehyde, a similar molecule to PyCHO as the monomer. (b) Circularly polarized luminescence and (c) single-molecule force spectroscopy characterizations of the control polymer in DMSO and water, respectively.

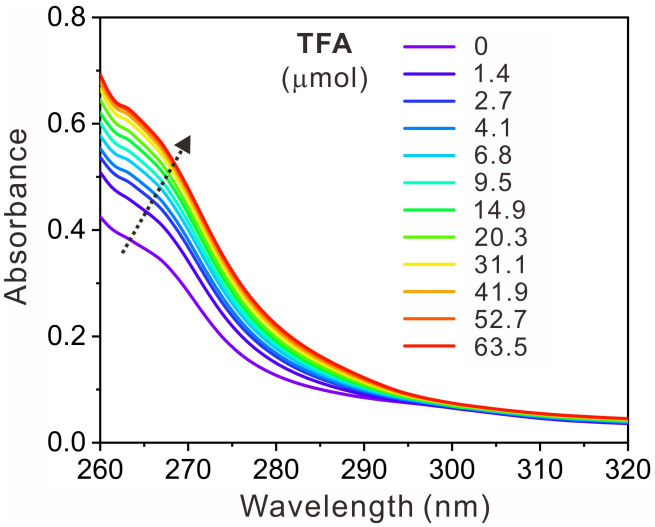

Figure S10. UV-vis spectra of WADP in DMSO (0.125 g L^{-1}) with different contents of trifluoroacetic acid (TFA).

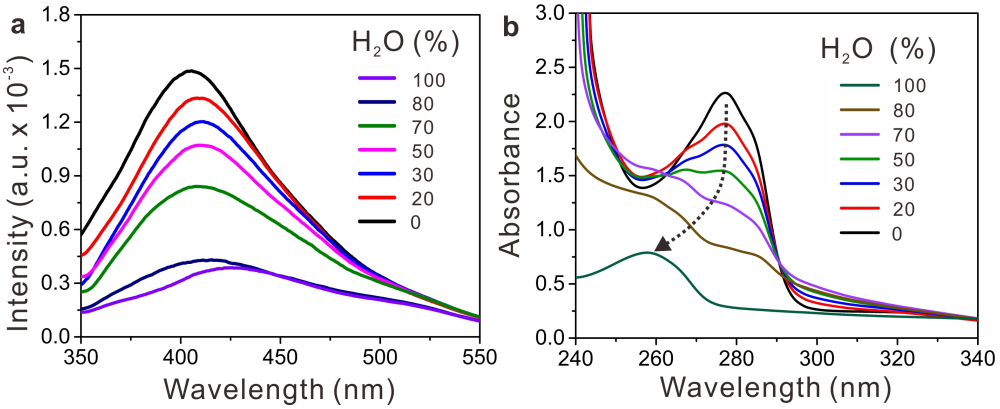

Figure S11. (a) The fluorescence and (b) UV spectra of WADP in THF with different weight ratios of water.

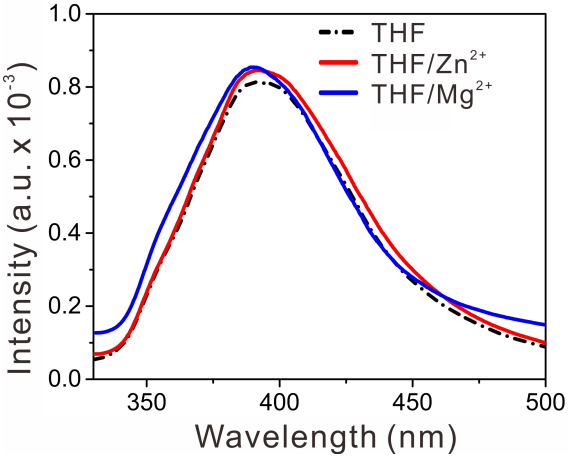

Figure S12. Fluorescence spectra of WADP in pure and Zn^{2+} (or Mg^{2+})-containing THF.

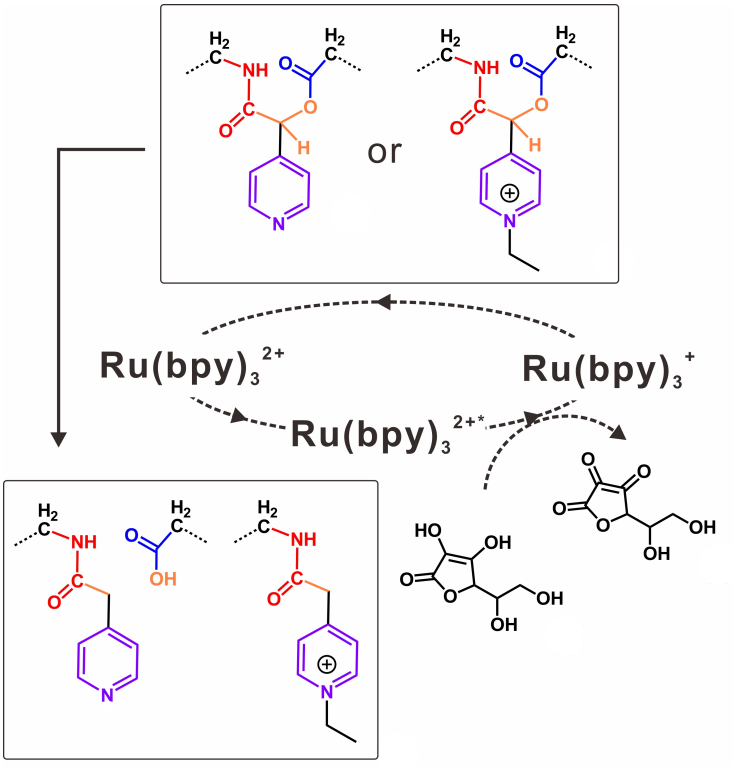

Figure S13. The photodegradation mechanism of small molecules and polymers with the catalysis of tris(bipyridine) ruthenium(II) chloride (Ru(II)) and ascorbic acid under blue light irradiation.

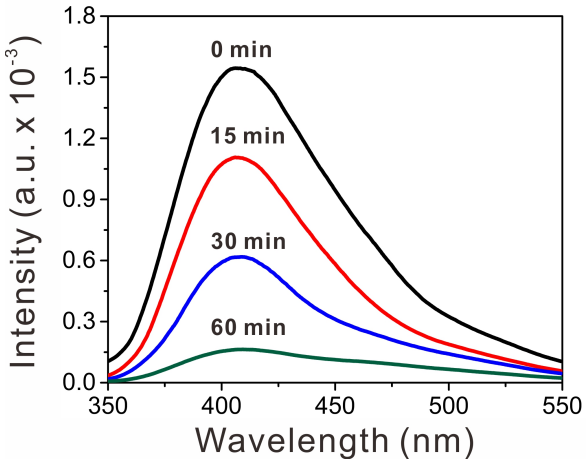

Figure S14. Fluorescence spectra of degradation products in THF with different reaction times.

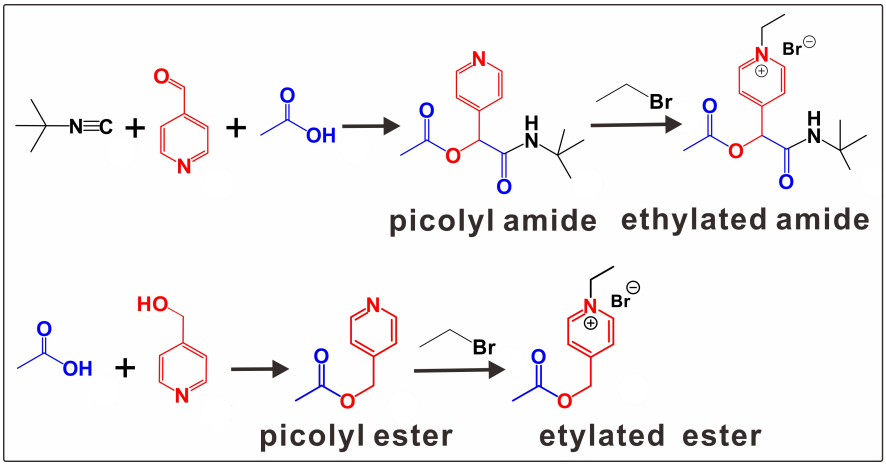

Figure S15. Synthesis of four small model molecules, including the amide, ethylated amide, picolyl ester, and ethylated ester.

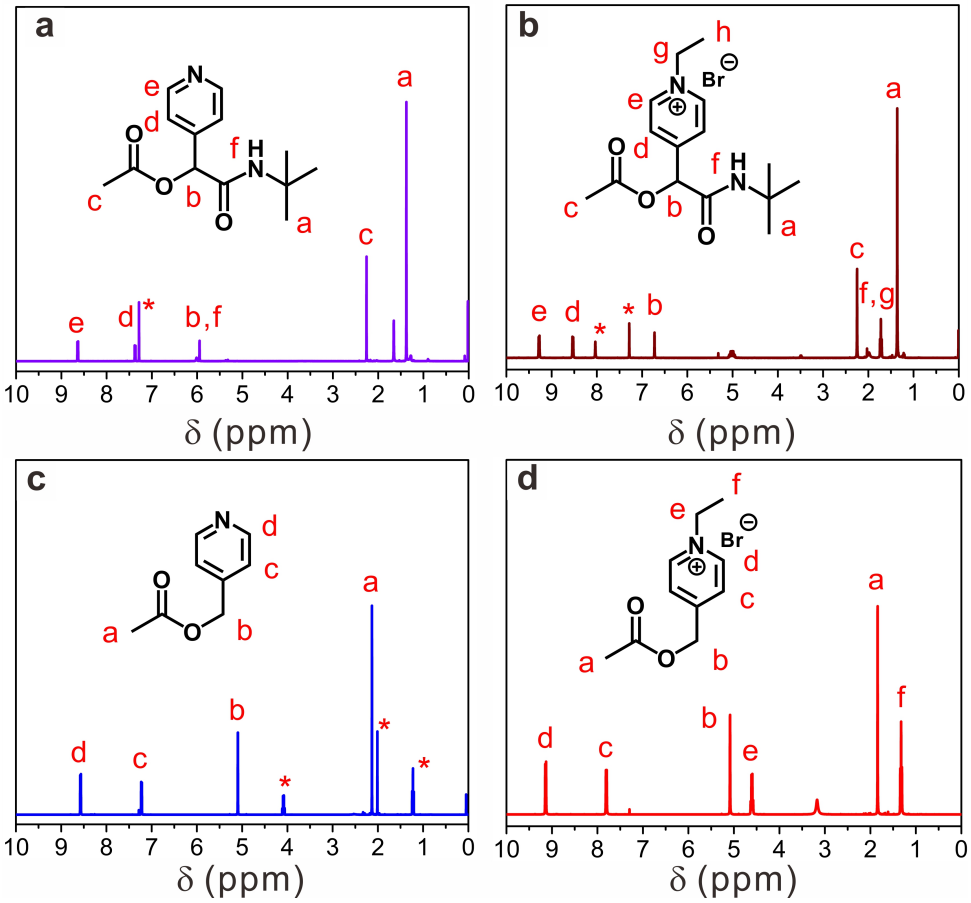

Figure S16. ^{1}H-NMR spectra of small model molecules including (a) amide, (b) ethylated amide, (c) picolyl ester, and (d) ethylated picolyl ester in DMSO-d6.

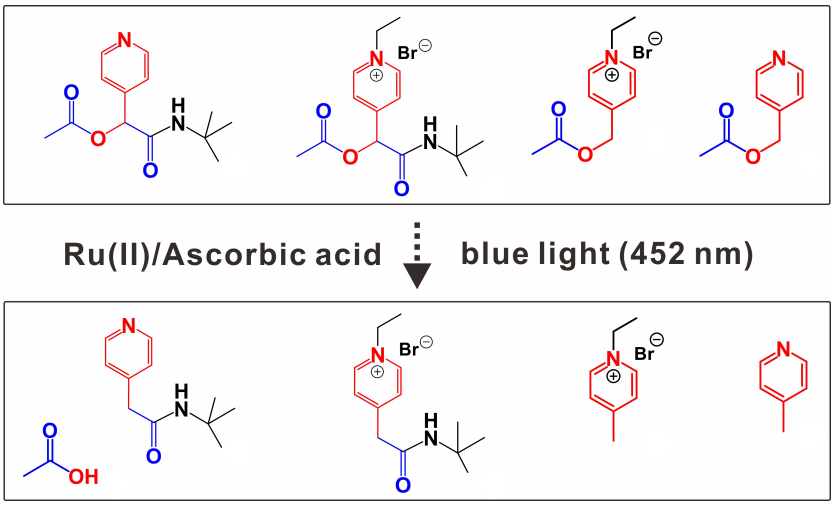

Figure S17. Degradation of small model molecules.

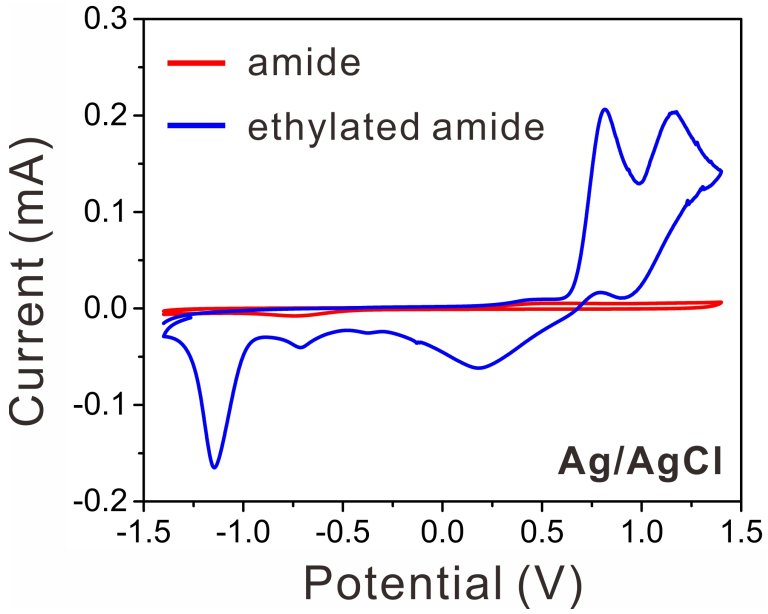

Figure S18. Cyclic voltammetry characterization of the model molecules of the amide and ethylated amide. The cyclic voltammetry was performed at room temperature by using a CHI-660E electrochemical workstation. A carbon electrode was applied as the working electrode. A Pt wire constituted the counter electrode, and an Ag/AgCl electrode served as the reference electrode. The supporting electrolyte was 0.1 M lithium perchlorate in dry acetonitrile. The solution was deoxygenated by bubbling argon gas through the solution for 15 min. The potential was swept from -1.5 to 1.5 V with the sweep rate of 100 mV/s to record the current-voltage curves.

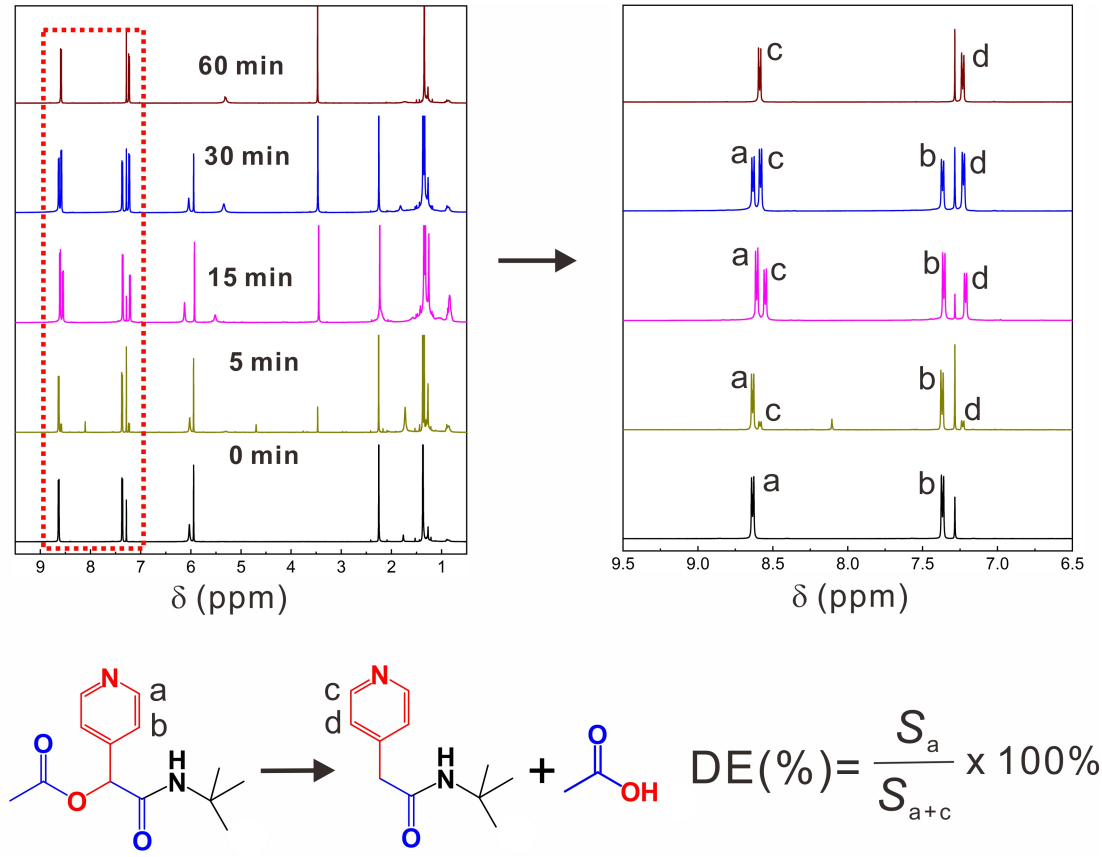

Figure S19. Calculating the degradation efficiency of the model amide with different irradiation time.

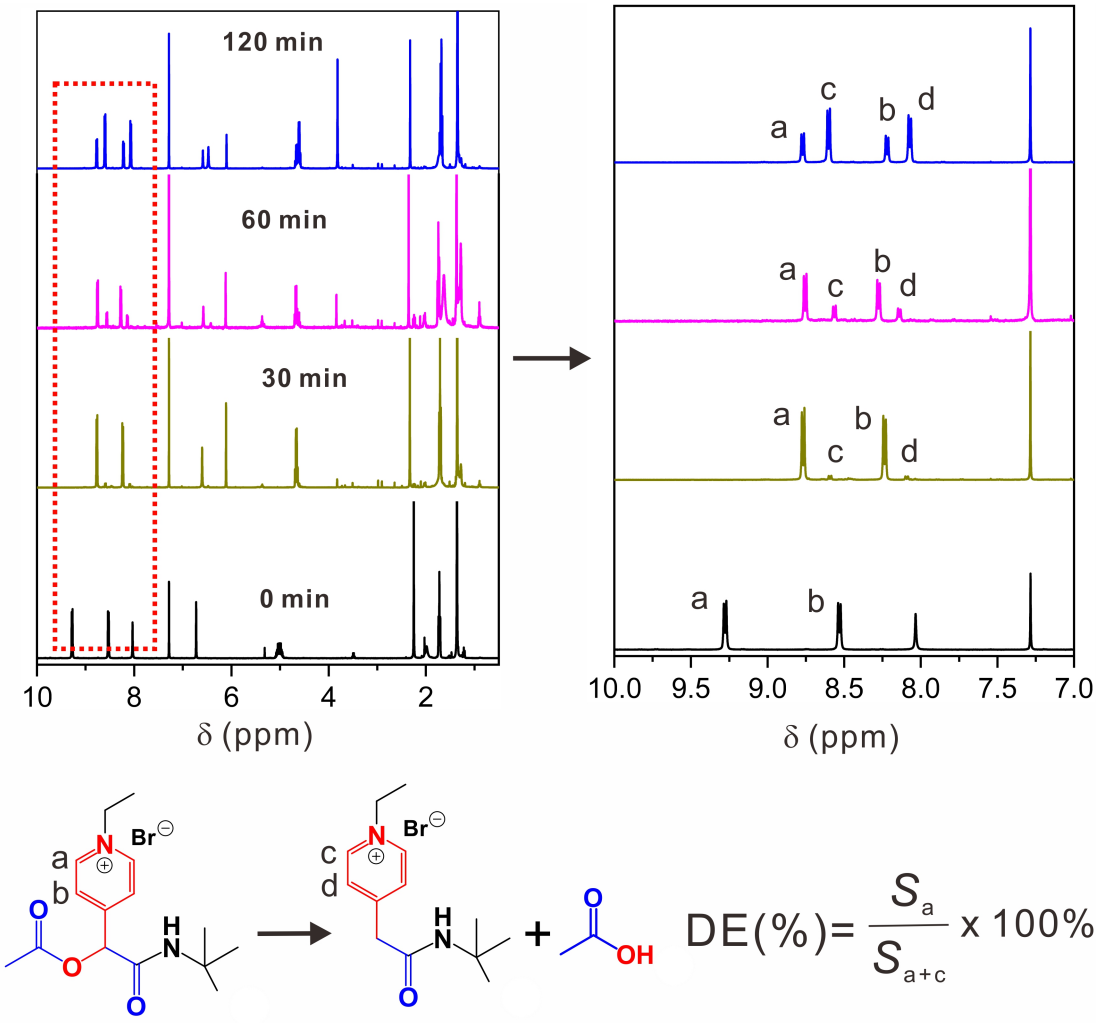

Figure S20. Calculating the degradation efficiency of the ethylated amide with different irradiation time.

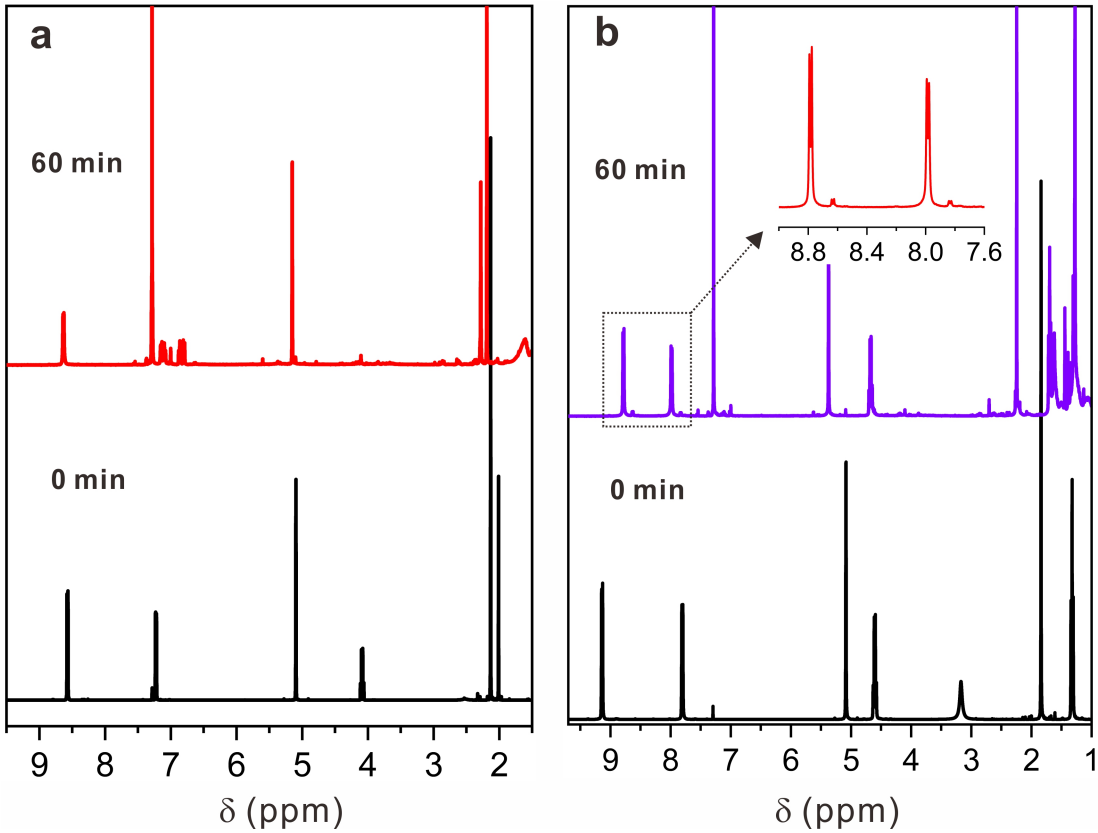

Figure S21. ^{1}H-NMR spectra of the (a) picolyl ester and (b) ethylated ester before and after 60 min of visible-light irradiation. The degradation efficiency of ethylated ester in (b) is calculated from the area ratio of peaks between 8.6 and 8.8 ppm, or 7.8 and 8.0 ppm.